

## Alkaline pH, Membrane Potential, and Magnesium Cations Are Negative Modulators of Purine Nucleotide Inhibition of H<sup>+</sup> and Cl<sup>-</sup> Transport Through the Uncoupling Protein of Brown Adipose Tissue Mitochondria

Petr Ježek,<sup>1,2</sup> Josef Houštěk,<sup>1</sup> and Zdeněk Drahotá<sup>1</sup>

Received November 5, 1987; revised March 28, 1988

### Abstract

Modulators of purine nucleotide (PN) inhibition of H<sup>+</sup> and Cl<sup>-</sup> transport mediated by the uncoupling protein (UP) of brown adipose tissue (BAT) mitochondria were studied: Alkalinization strongly diminishes GDP inhibition of H<sup>+</sup> transport ( $\Delta \log IC_{50} = -\Delta pH_{out}$ ), while more intensive inhibition of Cl<sup>-</sup> transport is only slightly altered. Higher  $\Delta\psi$  decreases GDP inhibition of H<sup>+</sup> transport. Mg<sup>2+</sup>, but not palmitoyl-CoA, decreases PN inhibitory ability.

Simulations of conditions similar to those found in BAT cells in the resting state and in the thermogenic state showed that three factors act in concert: pH, Mg<sup>2+</sup>, and free fatty acids (FFA): (a) with endogenous FFA present and 2 mM ATP and 0.5 mM AMP (pH 7.1), H<sup>+</sup> transport was inhibited by 95% in the absence of Mg<sup>2+</sup>, while by 60% with Mg<sup>2+</sup>; (b) 0.5 mM ATP and 1 mM AMP, H<sup>+</sup> transport was inhibited by 40% without Mg<sup>2+</sup> and by 30% with Mg<sup>2+</sup>. State b thus represents a model thermogenic state, while state a represents a resting state. However, the latter state *in vivo* must be accomplished either by combustion or FFA or by elimination of Mg<sup>2+</sup> to attain a total inhibition of H<sup>+</sup> transport (cf. a).

The model of UP possessing two independent channels, an H<sup>+</sup> channel and a Cl<sup>-</sup> channel, controlled from a single PN-binding site is supported by independent kinetics by different pH dependence of H<sup>+</sup> and Cl<sup>-</sup> transport, and by a lower sensitivity of H<sup>+</sup> transport to PN inhibition.

**Key Words:** Brown adipose tissue mitochondria; uncoupling protein; regulation of thermogenesis; modulators of purine nucleotide inhibition; magnesium.

<sup>1</sup>Institute of Physiology, Czechoslovak Academy of Sciences, Vídeňská 1083, 142 20 Prague 4, Czechoslovakia.

<sup>2</sup>To whom correspondence should be addressed.

## Introduction

The molecular mechanism of thermogenesis in brown adipose tissue (BAT)<sup>3</sup> has been well established, and the unique dimeric integral protein ( $2 \times 33,000$ ) of the inner membrane of BAT mitochondria—the uncoupling protein (UP)—has been recognized as the site of free energy conversion to heat (Nicholls, 1979; Nicholls and Locke, 1984; Himms-Hagen, 1985; Cannon and Nedergaard, 1985a,b). UP forms a gated  $H^+$  channel across the inner membrane (Strieleman *et al.*, 1985a,b; Klingenberg and Winkler, 1985) and allows for controllable uncoupling of BAT mitochondria. Free energy of  $\Delta/\tilde{\mu}_{H^+}$  is thus transformed into heat. In addition to  $H^+$  (or  $OH^-$ ), UP also conducts halide anions, especially  $Cl^-$  (Nicholls and Lindberg, 1973), that are probably translocated by a structurally different pathway (Kopecký *et al.*, 1984).

Both channels of UP close after sufficient binding of purine nucleotides (PN) to the PN-binding site located at the outer surface (Nicholls and Lindberg, 1973; Nicholls *et al.*, 1974; Heaton *et al.*, 1978; Kopecký *et al.*, 1984, 1987; Strieleman *et al.*, 1985a,b; Klingenberg and Winkler, 1985). Each dimeric unit of UP bears one such site (Lin and Klingenberg, 1982). PN binding strongly decreases with increasing pH (Lin and Klingenberg, 1982; Klingenberg, 1984). It was also found by the indirect method that the inhibitory ability of PN nucleotides decreases with increasing pH (Nicholls, 1974).

Full coupling of respiring BAT mitochondria (e.g., the highest proton-motive force) can be attained only in the simultaneous presence of GDP and bovine serum albumin (BSA), which remove free fatty acids (FFA) from membranes (Nicholls, 1974). The stimulatory effect of FFA on  $H^+$  transport in BAT mitochondria differs qualitatively from the trivial uncoupling effect of FFA observed in other types of mitochondria lacking UP (Locke *et al.*, 1982; Rial *et al.*, 1983) and was present even in the reconstituted system (Strieleman *et al.*, 1985b). However, removal of FFA does not affect the function of the  $Cl^-$  channel (Nicholls and Lindberg, 1973).

The detailed events taking place during the acute regulation of thermogenesis remain unclear. The key role is probably played by FFA (Nicholls and Locke, 1984) and by ATP (La Noue *et al.*, 1986). Norepinephrine-stimulated lipolysis leads to the elevation of FFA, which are subsequently catabolized by beta-oxidation in the matrix and could simultaneously serve as a messenger interacting with UP. A decrease in the cytosolic ATP

<sup>3</sup>Abbreviations: BAT, brown adipose tissue; DASMPI, 2-(*p*-dimethylaminostyryl)-(1-methylpyridinium)iodide; FFA, free fatty acids; L.S., light scattering; PN, purine nucleotides; TES, *N*-tris-hydroxymethyl-methyl-2-aminoethane sulfonic acid; UP, uncoupling protein.

was also found in BAT cells after norepinephrine stimulation (La Noue *et al.*, 1986), which emphasizes a regulation by PN. It is not known which of those regulatory levels is primary or whether both of them are necessary.

In addition, other factors (modulators) can affect the purine nucleotide inhibition. First, the values of intermembrane space pH are not known; therefore, one cannot decide whether 0.5 mM ATP found in the cytosol of BAT cells in the norepinephrine-stimulated state (La Noue *et al.*, 1986) allows H<sup>+</sup> transport. Alkalinization in the cytosol was even suggested as a primary initiator of thermogenesis (Chinet *et al.*, 1978). Long-chain acyl-CoA esters (Cannon *et al.*, 1977; Strielemann and Shrago, 1985) and the local membrane potential (Nicholls *et al.*, 1984) were also suggested as modulators decreasing PN inhibition.

In view of a complete lack of studies comparing the various possible regulators of thermogenesis under identical conditions, we tried to do this using our direct method for measurement of H<sup>+</sup> transport through UP in intact BAT mitochondria. It enabled us to evaluate alkaline pH and increasing Mg<sup>2+</sup> concentration as the main modulators decreasing PN inhibition of UP ion transport and high  $\Delta\psi$  as a factor decreasing the coupling. We further demonstrated that regulation by FFA and regulation by PN are equally meaningful. In addition, we present here a model of UP functional domains derived from the data. A part concerning the palmitoyl-CoA effect has already been published as a congress report (Ježek and Houštěk, 1986).

## Materials and Methods

Antimycin, oligomycin, rotenone, valinomycin, nigericin, BSA (FFA free), and Na salts of GDP, GMP, ATP, and AMP were purchased from Sigma (USA); all other chemicals were of analytical grade. 2-(*p*-dimethylaminostyryl-(1-methylpyridinium)iodide (DASMPI) was a kind gift from Prof. J. Rafael (University of Heidelberg, Heidelberg, FRG).

Syrian hamsters weighing > 100 g were exposed for at least 3 weeks to 5°C and then used for the preparation of mitochondria according to the method described by Hittelman *et al.* (1969). Hamster liver mitochondria were prepared by the usual procedure.

### *Measurement of UP Ion Transport in Intact Mitochondria*

While H<sup>+</sup> transport was indicated directly by changes in external pH, simultaneous Cl<sup>-</sup> transport was measured indirectly as swelling or contraction of BAT mitochondria in KCl using 90° light scattering for indication of volume changes. A combination pH electrode (Beckman no. 39505) was

placed in a constant-temperature cuvette (25°C) of a Perkin-Elmer MPF 3A fluorometer equipped with an analogue fast-response output unit and with a stirrer. Two polarizers (Polaroid, UK) were imposed in parallel orientation into the incident and scattered-light beam. The pH electrode output was connected to a Keithley 614 electrometer (input resistance,  $10^{14}$   $\Omega$ ) with a compensator making it possible to monitor at 2 mV full scale (0.03 pH) on a dual-channel recorder. In some experiments, fluorescence of DASMPI was employed for indication of  $\Delta\psi$  courses according to the method described by Mewes and Rafael (1980). A decrease of DASMPI fluorescence indicate a decrease in the negative charge inside.

Both possible directions of passive ion fluxes were induced by imposing a  $K^+$  diffusion potential:

1. *Valinomycin-Induced  $H^+$  Extrusion in Isotonic Potassium Salts.* BAT mitochondria (1–3 mg protein/ml) were suspended in 150 mM KCl or 110 mM  $K_2SO_4$  containing 1–3 mM K-TES, Tris-TES or Tris-Cl of appropriate pH, 8  $\mu$ M rotenone, 1  $\mu$ M antimycin, and 2.5  $\mu$ M oligomycin. After a defined time interval 0.7–1  $\mu$ g valinomycin/mg protein was added. The addition resulted in a rapid  $H^+$  extrusion from mitochondria followed by swelling of mitochondria when  $Cl^-$  anions were present (in KCl, Fig. 1). The time courses of these processes in KCl are not synchronous— $H^+$  extrusion is faster than swelling—and both can be totally inhibited by GDP (Fig. 1) and do not exist in any other type of mitochondria lacking UP. This demonstrates the participation of UP in both processes, and that  $H^+$  extrusion is a suitable direct method of measurement of  $H^+$  transport through UP in intact BAT mitochondria (cf. Kopecký *et al.*, 1984, 1987; Houštek *et al.*, 1987). The  $\Delta\psi$ -sensitive fluorescence probe DASMPI indicates a decrease in the negative charge inside induced valinomycin addition and terminated at the end of swelling, which is also prevented by GDP (Fig. 1). It is worth noting that albumin almost completely inhibits  $H^+$  extrusion (Kopecký *et al.*, 1984).

2. *Valinomycin-Induced  $H^+$  Uptake into KCl-Loaded Mitochondria.* To generate a reverse  $H^+$  flow, analogous to the  $H^+$  influx occurring during thermogenesis *in vivo*, we developed another way of inducing  $H^+$  transport. BAT mitochondria at 1 mg/ml were preloaded with a 150 mM KCl medium by 20 min incubation in the absence of valinomycin at room temperature under vigorous stirring. Fully swollen mitochondria were then sedimented at 10,000 *g* and 0°C, and resuspended to a dense suspension in a KCl medium. Aliquots of this suspension were transferred to the cuvette containing isotonic sucrose so that the final concentration was 1.0–1.3 mg protein/ml. After 15 sec, valinomycin was added. This causes a rapid alkalization of the external medium and mitochondrial contraction when KCl-loaded

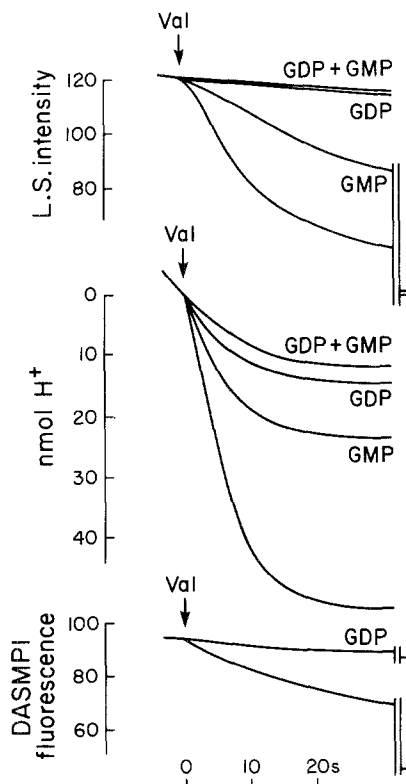


**Fig. 1.** Simultaneous records of  $H^+$  extrusion (middle traces) and either swelling (top traces) or DASMPI fluorescence response (bottom traces) induced by valinomycin in 150 mM KCl, 2 mM K-TES (pH 7.05) with or without GDP and GMP (210  $\mu$ M), or with both. BAT mitochondria at 1 mg/ml were used, and valinomycin was added after 30 sec of incubation. L.S., light scattering.

mitochondria are used, but not with unloaded (intact) BAT mitochondria (Fig. 2A) (Drahota *et al.*, 1985). DASMPI fluorescence indicates a decrease in positive charge inside.

When hamster liver mitochondria were loaded with KCl by means of the same procedure, a negligible  $H^+$  uptake was observed with valinomycin. The existence of sufficient gradients for driving  $H^+$  uptake was confirmed in this case by the natural  $K^+/H^+$  exchanger nigericin, which induces massive  $H^+$  uptake (Fig. 2B). Neither of the ionophores induces a rapid contraction of KCl-loaded liver mitochondria as is observed with KCl-loaded BAT mitochondria. Moreover, GDP inhibits both  $H^+$  uptake and contraction (Fig. 2A). All of these results demonstrate the participation of UP in the

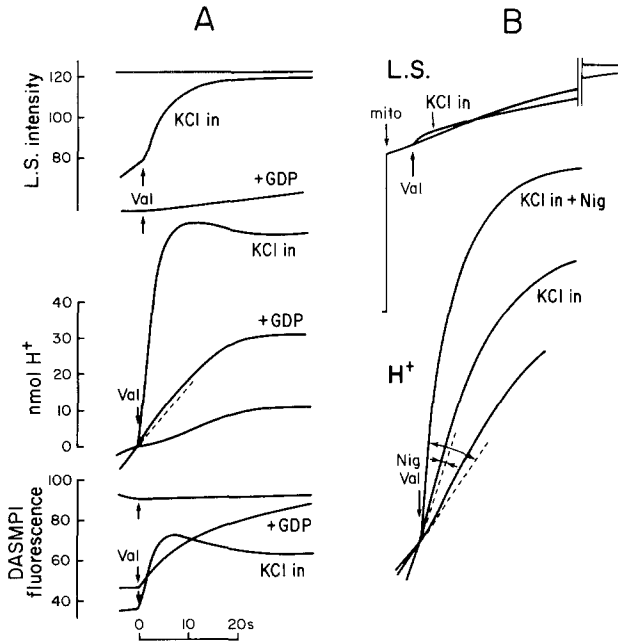


**Fig. 2.** Reversed ionic fluxes in KCl-loaded BAT mitochondria (A) and liver mitochondria. (B) Valinomycin-induced contraction, H<sup>+</sup> uptake, and  $\Delta\psi$  changes in KCl-loaded mitochondria with and without GDP (400  $\mu$ M) and in unloaded (intact) mitochondria were measured after a 15-sec equilibration of mitochondria with 250 mM sucrose medium. Note that H<sup>+</sup> uptake into KCl-loaded liver mitochondria occurs only with nigericin (differences between rates before and after the ionophore are indicated by curved arrows).

process of H<sup>+</sup> uptake and partly in the observed contraction. We used this method to estimate  $\Delta\psi$  dependence of H<sup>+</sup> transport. In this case, sucrose was replaced with a series of choline chloride–KCl mixtures maintaining 150 mM Cl<sup>-</sup> with various K<sup>+</sup> concentrations. Applied K<sup>+</sup> diffusion potentials were estimated according to the Nernst equation on the assumption that 150 mM KCl was in the matrix and that the low concentration of K<sup>+</sup> outside (calculated from known volumes of added mitochondrial samples) did not increase before valinomycin was added. Therefore, the estimates represent the upper limit.

In both types of measurement, small aliquots of HCl were added for calibration after each trace record. The initial rate ( $v_0$ ) in nmol H<sup>+</sup>/min/mg protein was obtained by subtracting the rate before valinomycin addition from that after it. Swelling rates were calculated analogously and were expressed as percent of initial light-scattering intensity ( $I_0$ ) in %  $I_0$  min<sup>-1</sup>.

## Results

### *Effect of External pH on the Inhibition of Transport by Purine Nucleotides*

Figure 3A and B shows the effect of external pH on GDP inhibition of  $H^+$  extrusion. With increasing pH, the corresponding titration curves are shifted toward higher GDP concentrations. Parameters of half-maximum inhibition<sup>4</sup>  $IC_{50}(H^+)$  and  $IC_{50}(Cl^-)$  increase considerably within the pH range of 6.2–8.2 (Table I). In the case of  $H^+$  extrusion, the following relationship is approximately true:

$$\Delta \log IC_{50}(H^+) = -\Delta pH_{out} \quad (1)$$

The slope of the corresponding relationship obtained by linear regression from the experimental data is 1.1 ( $r^2 = 0.92$ ) (Fig. 3B). GDP inhibition of  $H^+$  extrusion in  $K_2SO_4$  also exhibits a similar pH dependence (not shown). In the case of simultaneously measured  $Cl^-$  transport, however, the observed linear relationship between  $\log IC_{50}(Cl^-)$  and pH change exhibits a lower slope of 0.63 ( $r^2 = 0.93$ ). The contribution of GDP-insensitive residual transport was subtracted here (Fig. 3B and Table I). At all pH values,  $Cl^-$  transport was more sensitive to GDP (Table I), ATP, AMP and GMP (see below) than was  $H^+$  transport. The following values were found for ATP (in

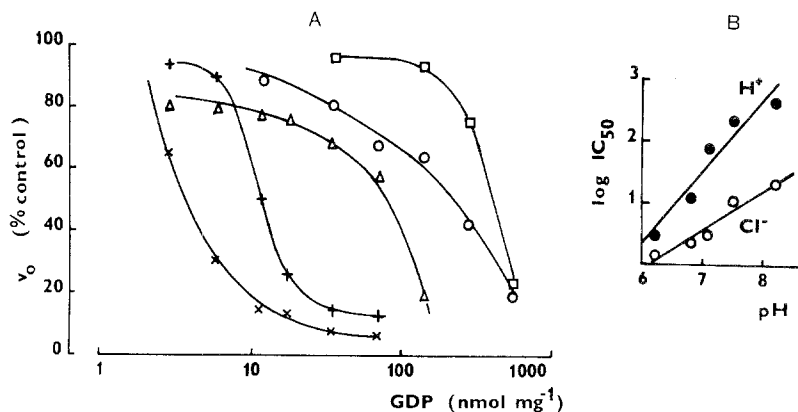


Fig. 3. (A) Initial rates of valinomycin induced  $H^+$  extrusion in 150 mM KCl and 2 mM K-TES, as functions of GDP concentrations at different pH: (x) 6.2, (+) 6.8, ( $\Delta$ ) 7.1, ( $\circ$ ) 7.5, and ( $\square$ ) 8.2. Used were 3 mg protein ml<sup>-1</sup> of BAT mitochondria. (B)  $IC_{50}(H^+)$  and  $IC_{50}(Cl^-)$  [in nmol GDP (mg protein)<sup>-1</sup>] as functions of pH derived from GDP titrations of valinomycin-induced  $H^+$  extrusion ( $\bullet$ ) and the accompanying swelling in KCl ( $\circ$ ).

<sup>4</sup> $IC_{50}(H^+)$  designates an inhibitor concentration required for a decrease of the transport rate to 50%.

**Table I.** pH Dependence of  $IC_{50}(H^+)$  and  $IC_{50}(Cl^-)$  for GDP<sup>a</sup>

Transport	$IC_{50}$ in nmol GDP (mg protein) <sup>-1</sup> estimated at pH:				
	6.2	6.8	7.1	7.5	8.2
H <sup>+</sup>	3	12	79	220	440
Cl <sup>-</sup>	1.4	2.1	3.0	10.4 <sup>b</sup>	20 <sup>b</sup>

<sup>a</sup>Valinomycin-induced H<sup>+</sup> extrusion and swelling of BAT mitochondria were measured as described in *Materials and Methods*, with the exception that 2 mM K-TES adjusted to appropriate pH was included and 3 mg protein ml<sup>-1</sup> were used.

<sup>b</sup> $IC_{50}$  values were calculated with regard to the possible participation of GDP-insensitive Cl<sup>-</sup> transport unmasked by alkaline pH (cf. Warhurst *et al.*, 1982). Nonzero levels at high GDP concentrations were subtracted from controls and these differences were taken as 100%.

nmol/mg protein):  $IC_{50}(H^+) = 30$  at pH 6.8, and 70 at pH 7.0; and  $IC_{50}(Cl^-) = 4.6$  at pH 6.8, and 15 at pH 7.0.

#### *Inhibition by Addition of GMP and GDP*

Purine nucleoside monophosphates exhibits a lower binding affinity for UP than di- and triphosphates (Lin and Klingenberg, 1982) and inhibit UP

**Table II.** Parameters of GDP, GMP inhibition, and double inhibition by GDP plus GMP (all values expressed in  $\mu M$ )<sup>a</sup>

Parameter	Cl <sup>-</sup> transport		H <sup>+</sup> transport	
$IC_{50}^{GMP}$	60		200	
$IC_{50}^{GDP}$	6.7	5.0 <sup>c</sup>	30.5	29 <sup>c</sup>
$AIC_{50}^{GDP}$ at 105 $\mu M$ GMP <sup>b</sup>	16		~ 32	
$AIC_{50}^{GDP}$ at 210 $\mu M$ GMP <sup>b</sup>	26		45	
$K_d^{GDP}$	5.2 $\pm$ 0.2		7 $\pm$ 1	
$K_d^{GMP}$	68 $\pm$ 7		~ 70	

<sup>a</sup>Measured in 150 mM KCl, 1 mM K-TES pH 7.05 at 1 mg protein/ml. Dixon plots were constructed (cf. Fig. 4) and the dissociation constants were calculated according to a simple model assuming the proportionality between the occupancy of PN-binding site and the number of closed channels (in the case of H<sup>+</sup> transport, the proportionality was assumed only above the upper limit of the latent concentration range):

$$K_d^{GDP} = 1/a_1 \quad \text{and} \quad K_d^{GMP} = [GMP]/(a_0 - 1)$$

where  $a_0$  and  $a_1$  designate the intercepts and slopes, respectively, of Dixon plots for GDP inhibition in the presence of GMP at concentration GMP. The latent concentration range was subtracted from the intercept in the case of H<sup>+</sup> transport.

<sup>b</sup>The symbol  $AIC_{50}^{GDP}$  designates the apparent GDP concentration required for a degree of the remaining transport activity with given GMP to 50%.

<sup>c</sup>Derived from the slopes of linear Dixon plots. Standard error was calculated from the goodness of the linear regression fit.

<sup>d</sup>Derived from the intercepts of Dixon plots. The latent concentration range was subtracted from the intercept in the case of the H<sup>+</sup> transport.

<sup>e</sup>Derived from the linear Dixon plot as a cross section of the level  $w^{-1} = 2$ .



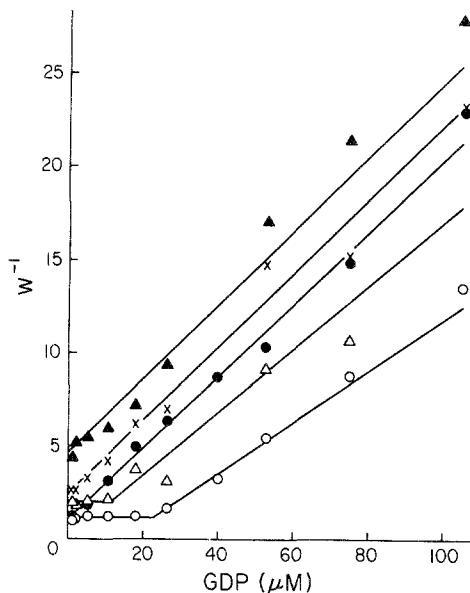


**Fig. 4.** Dixon plots for GDP titrations of  $H^+$  extrusion ( $\circ$ ,  $\Delta$ ) and swelling ( $\bullet$ ,  $\times$ ,  $\Delta$ ) in 150 mM KCl and 1 mM K-TES, pH 7.05, in the absence of GMP ( $\circ$ ,  $\bullet$ ), in the presence of 105  $\mu$ M GDP ( $\times$ ) and 210  $\mu$ M GMP ( $\Delta$ ,  $\blacktriangle$ ). Linear regression by the least-squares method also included points measured at 210  $\mu$ M GDP. All fits yielded  $r^2$  values  $> 0.9$ . Each point represents the average of two measurements.

transport much less effectively (Nicholls *et al.*, 1974). In addition to GDP, we employed GMP as a model nucleotide and estimated the inhibitory parameters of their respective single inhibition and GDP inhibition at sub-maximum GMP levels (Figs. 1 and 4, and Table II). The values of half-maximum inhibition are  $\sim 10$  times higher for GMP than for GDP (Table II). The values of half-maximum inhibition are  $\sim 10$  times higher for GMP than for GDP (Table II). GMP and GDP act apparently in an additive manner (Fig. 1). More precisely, linear Dixon plots of GDP inhibitory data obtained at various submaximum GMP concentrations are parallel and are shifted to a lower GDP concentration range (Fig. 4 and Table II). As the same effect is observed with the physiological ATP-AMP couple (not shown), one cannot expect any activation of  $H^+$  transport through UP by a simple elevation of AMP level without a simultaneous decrease in ATP.

One important feature of GDP inhibition should be pointed out. There exists a latent concentration range in which GDP binds to UP, but does not inhibit  $H^+$  transport (cf. Kopecký *et al.*, 1987; Ježek *et al.*, 1988). At pH 7.05, it is indicated by a constant part of the Dixon plot up to 20  $\mu$ M GDP (Fig. 4). The simultaneous presence of 210  $\mu$ M GMP reduces this range to  $\sim 10$   $\mu$ M.

The PN-binding site exhibits a single dissociation constant for the binding as calculated according to the simple model assuming the proportionality between the occupancy and the number of closed channels above the upper limit of the latent concentration range (Table II).

#### *Effect of $\Delta\psi$ on $H^+$ Transport Rates and on GDP Inhibition*

Using  $H^+$  uptake into KCl-loaded BAT mitochondria, we tried to evaluate the effect of  $\Delta\psi$ . The  $\Delta\psi$  dependence in controls shows a break near 20 mV and continues as a linear relationship up to 120 mV (Fig. 5A). When 38.5 nmol GDP/mg protein is present, the  $\Delta\psi$  dependence has the following shape: zero levels of  $H^+$  uptake are observed up to 20 mV; a nearly biphasic curve is found above 20 mV with a break at 80 mV, above which the dependence shows an almost equal slope as in the control.

Calculation of GDP inhibition from these relationships showed that it slightly decreases with increasing  $\Delta\psi$  when assuming that the whole extent of  $H^+$  uptake was due to UP activity (Fig. 5B). Up to 35 mV, 38 nmol GDP/mg protein inhibits fully; at 40 mV, GDP blocks 93% and, at 120 mV, 68% of  $H^+$  uptake activity. When subtracting the  $\Delta\psi$  dependence measured with GDP from the control, we obtained the GDP-sensitive part of  $H^+$  transport as related to  $\Delta\psi$ . Such a dependence approaches saturation at  $> 100$  mV (Fig. 5A).

#### *Effect of Palmitoyl-CoA*

In further experiments, we tested the possibility of whether palmitoyl-CoA, another suggested modulator of PN inhibition, affects GDP inhibition of  $H^+$  extrusion and swelling in KCl. The equilibration of GDP with BAT mitochondria lasted 25 sec. Palmitoyl-CoA was then added and valinomycin was added after a further 35 sec. Controls were swollen to the same initial volume as mitochondria with palmitoyl-CoA at the moment of valinomycin addition. The results showed that palmitoyl-CoA causes no changes in the shape of GDP titrations and no shifts in  $IC_{50}$  values in the case of both UP transport activities when estimated at pH 6.8 as well as at pH 7.1 (not shown). The simultaneous addition of palmitoyl-CoA and GDP did not lead to any detectable effect. Control titrations were performed, with mitochondria swollen to the volume occurring at the moment of valinomycin addition in the case of mitochondria with palmitoyl-CoA, as palmitoyl-CoA itself induces swelling. The rate of such palmitoyl-CoA-induced swelling of BAT mitochondria in the presence of 700 nmol GDP/mg protein increases with increasing palmitoyl-CoA concentrations in a similar way as such swelling of hamster liver mitochondria (Fig. 6). Moreover, it also occurs in other potassium salts and in choline chloride. The nonspecific nature of this process is thus demonstrated. The rate of palmitoyl-CoA-induced swelling

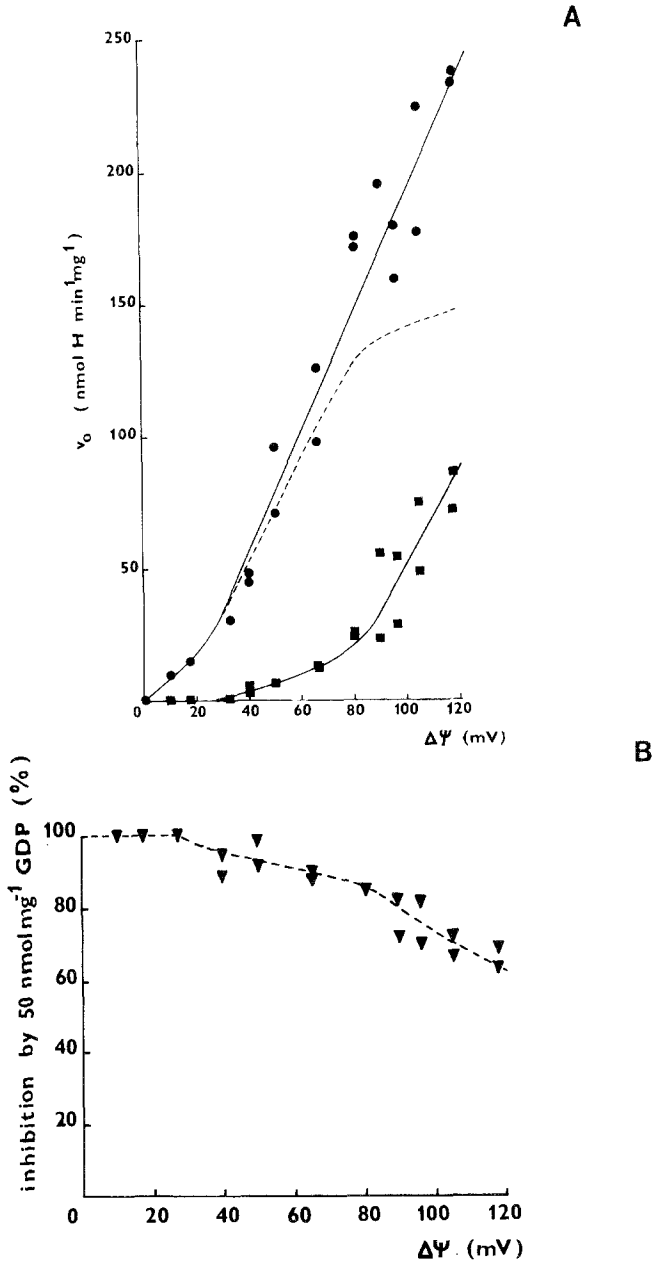


Fig. 5. (A) Initial rates of valinomycin-induced H<sup>+</sup> uptake into KCl-loaded BAT mitochondria as a function of Δψ at pH < 6.9: (●) without GDP and (■) with 50 μM GDP [38.5 nmol GDP (mg protein)<sup>-1</sup>]. The dotted line represents the subtraction of these curves. (B) GDP inhibitory ability as a function Δψ derived from data presented in A.

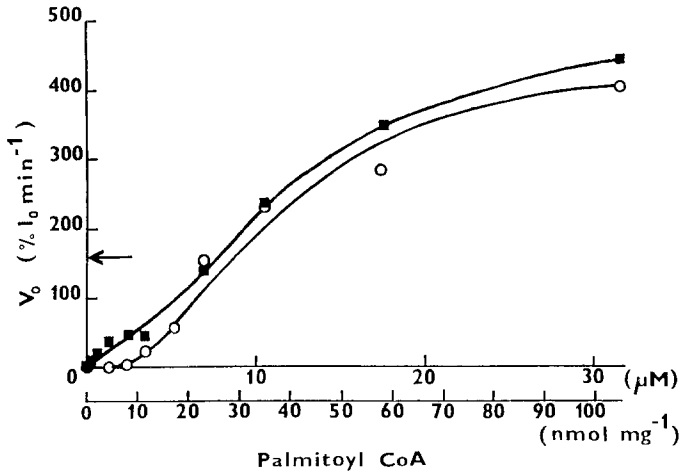


Fig. 6. Palmitoyl-CoA-induced swelling in KCl in the absence of valinomycin. Hamster liver mitochondria (O) or BAT mitochondria with 700 GDP (mg protein)<sup>-1</sup> (■) were used. The arrow indicates UP-dependent swelling of BAT mitochondria in KCl induced by valinomycin (GDP absent).

in KCl amounts to the rate of valinomycin-induced (i.e., UP-dependent swelling of BAT mitochondria in KCl at ~30 nmol palmitoyl-CoA/mg protein.

#### *Inhibition of H<sup>+</sup> Extrusion by Albumin*

It should be stressed that all the studied effects on H<sup>+</sup> transport and its regulation were measured in the presence of standard endogenous FFA levels. As illustrated in Fig. 7, it is not possible to measure passive H<sup>+</sup> fluxes

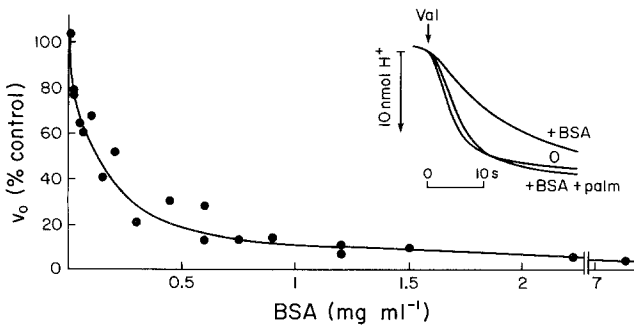


Fig. 7. Rates of the valinomycin-induced H<sup>+</sup> extrusion in 110 mM K<sub>2</sub>SO<sub>4</sub> as a function of bovine serum albumin (BSA) concentration at 1 mg BAT mitochondrial protein/(Inset) Restoration of H<sup>+</sup> transport by 250 μM K-palmitate at 2 mg BSA/ml.

in the absence of endogenous FFA. The presence of BSA at a concentration  $> 2$  mg/mg protein almost prevents  $H^+$  extrusion in  $K_2SO_4$  (Fig. 7). The addition of a greater amount of palmitate together with BSA enables  $H^+$  extrusion. Only a slightly reduced rate is observed in this case (inset in Fig. 7).

*UP Transport Activities Under Model Thermogenic and Resting Conditions:  
The Effect of  $Mg^{2+}$*

To demonstrate the effect of ATP and AMP on UP transport under a situation resembling conditions *in vivo*, we used the data of La Noue *et al.* (1986) regarding the cytosolic adenine nucleotide concentration in unstimulated and norepinephrine-stimulated states, and defined the state with the external concentration of 0.5 mM ATP and 1 mM AMP as a model thermogenic state and with 2 mM ATP and 0.5 mM AMP as a model resting state. ADP occurring *in vivo* at micromolar concentrations was neglected and endogenous FFA was always present. Thus, we tested the hypothesis explaining the decrease in the ATP level as an event initiating thermogenesis in BAT.

UP transport activities measured as  $H^+$  extrusion and swelling in KCl at pH 7.15 under these model conditions are compared in Fig. 8A. A 95% inhibition of  $H^+$  transport was found in the model resting state, whereas  $> 50\%$  of  $H^+$  transport activity was observed in the model thermogenic state. A much smaller difference between the states was observed in the case of  $Cl^-$  transport, which exhibited 17% and 33% of maximal activity, respectively.

The absence of  $Mg^{2+}$  in the above experiments could be seen as a non-physiological factor. Therefore, concentrations of  $MgCl_2$  equal to the concentrations of adenine nucleotides in the respective states were included in further experiments. In the model thermogenic state with 1.6 mM  $MgCl_2$ , the initial rates of  $H^+$  extrusion and  $Cl^-$  uptake increased by a factor of 1.21 and 1.96 in comparison with the respective rates in the absence of  $Mg^{2+}$  (Fig. 8B). Surprisingly, 2.5 mM  $MgCl_2$  in the model resting state also activates transport rates (40% of  $H^+$  transport and 25% of  $Cl^-$  transport activity with respect to the control without nucleotides are preserved). Thus, in spite of the presence of 2 mM ATP, both UP channels are not closed. When comparing the results of ATP titrations measured at the identical pH in the absence of  $Mg^{2+}$  (see above), we identified  $Mg^{2+}$  as a powerful modulator of PN inhibition. We further revealed that changes in external ATP found during norepinephrine activation of BAT cells are sufficient for opening the  $H^+$  channel, but the levels found in the resting state are not sufficient for attaining the closed state when  $Mg^{2+}$  is present. As measured in the presence of endogenous FFA, however, one can assume that the real resting state *in vivo* will be different from our model state, that FFA could be mostly catabolized, and that this would lead to the closed state of the UP  $H^+$  channel (cf. Fig. 7).

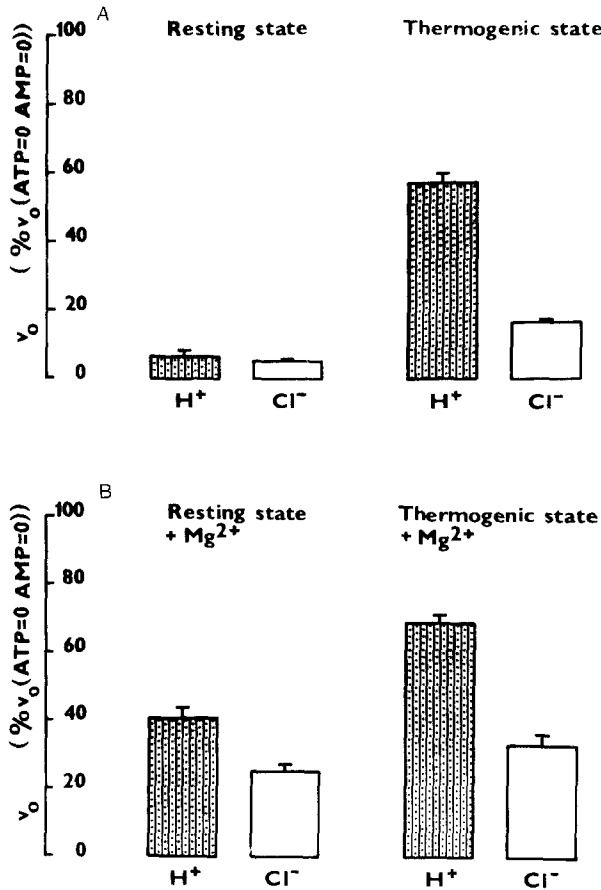


**Fig. 8.** Transport activities of the uncoupling protein under model thermogenic conditions (1 mM AMP and 0.5 mM ATP) or resting state conditions (0.5 mM AMP and 2 mM ATP) at pH 7.15 in the absence (A) and presence (B) of Mg<sup>2+</sup> in the amount equal to the total amount of nucleotides in 1.6 and 2.5 mM MgCl<sub>2</sub>, respectively. The columns represent averages from ten thermogenic condition or five nonthermogenic condition measurements on three mitochondrial preparations. The differences between the values in the presence and in the absence of Mg<sup>2+</sup> were significant at  $P < 0.0001$ .

*Effect of External pH on the Rates of H<sup>+</sup> and Cl<sup>-</sup> Transport Through the Uncoupling Protein*

In addition to all regulatory factors, the concentration of the transported substrate (i.e., H<sup>+</sup>) should control the H<sup>+</sup> transport rate. The pH dependence of the initial rate of valinomycin-induced H<sup>+</sup> extrusion in nonbuffered K<sub>2</sub>SO<sub>4</sub> exhibits an optimum near neutral pH, while, in nonbuffered KCl, almost a mirror image of the dependence in sulfate is found: rates are maximum at pH 5 and pH 9; a decrease of the activity was observed within the acid region with increasing pH. The lowest rates are observed at pH 8–8.8,

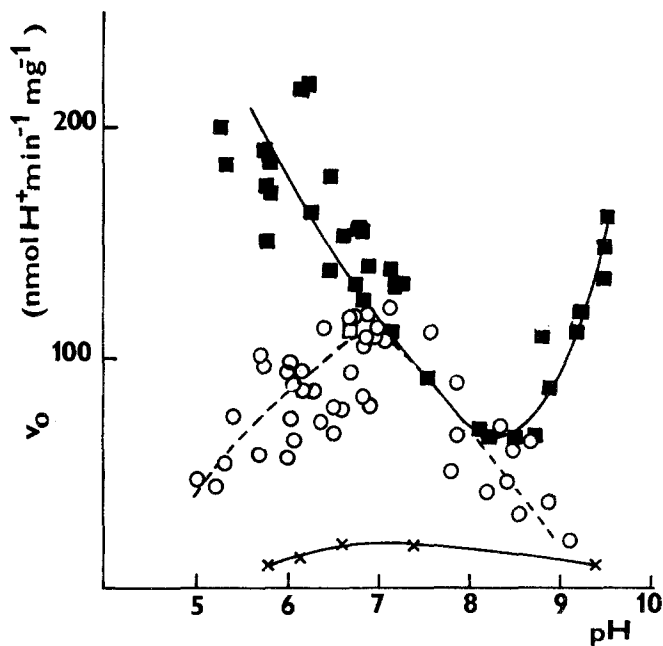


Fig. 9. pH dependence of initial rates of valinomycin-induced  $H^+$  extrusion in nonbuffered 150 mM KCl (■) and 110 mM  $K_2SO_4$  (○) measured at 1 mg protein  $ml^{-1}$ . pH values were derived from voltages on pH electrode compared by a calibration.

these being followed by an increase at extremely alkaline pH values (Fig. 9). Thus, when  $Cl^-$  transport proceeds simultaneously,  $H^+$  transport rates are higher in the acidic and higher alkaline pH regions in comparison with the rates obtained in the absence of  $Cl^-$  transport. When 1 mM KCl was included in the sulfate medium, no changes in pH dependence were found. This indicates that higher concentrations are required for the observed stimulation of  $H^+$  transport rates by KCl.

The pH dependence of  $Cl^-$  transport estimated either simultaneously or in a separate experiment in buffered KCl exhibited a negligible rate decrease with increasing pH (not shown).

## Discussion

### *Modulation of Purine Nucleotide Inhibition of the Uncoupling Protein-Mediated Transport*

Factors that affect PN inhibition are referred to here as modulators. Using the direct method for  $H^+$  transport measurement, we selected external pH and  $Mg^{2+}$  as the most important modulators of PN inhibition and  $\Delta\psi$  as

a feedback modulator of coupling, but we excluded palmitoyl-CoA and the related esters as possible regulators of UP function.

Palmitoyl-CoA cannot be a physiological modulator of PN inhibition because it neither changes the shape of GDP titrations nor shifts the  $IC_{50}$  at concentrations used here, which highly exceed the palmitoyl-CoA levels found *in vivo* (0.28 nmol/mg protein; see Norman and Flatmark, 1984). Moreover, its nonspecific effect on the inner membrane permeability rules out the original interpretations of experiments where swelling in KCl was reactivated by palmitoyl-CoA in the presence of GDP (Cannon *et al.*, 1977). It could also explain the observed changes in GDP binding to UP in the presence of palmitoyl-CoA (Cannon *et al.*, 1977; Strieleman and Shrago, 1985), as binding to swollen mitochondria can be altered.

External pH is a powerful modulator of PN inhibition of UP transport that sets the inhibitory ability of PN to the proper level. Therefore, any changes in pH homeostasis, but also in local pH (cf. Westerhoff *et al.*, 1984; Fergusson, 1985), would be sufficient to control BAT mitochondrial coupling. However, at present, no particular reaction is known to produce alkalization during the norepinephrine activation of BAT cells, and rather an acidification is expected (cf. Cannon and Nedergaard, 1985b). Therefore, we cannot judge whether alkalization in general serves as an initiator of thermogenesis. In BAT mitochondria, naturally occurring mosaic domains (cf. Westerhoff *et al.*, 1984) could be represented by the intermembrane space between the rich folding of the cristae in which pH values will differ from bulk cytosolic pH, as the latter was found to be heterogeneous (Slavík and Kotyk, 1984). We must also emphasize the dual role of protons in the mosaic zones. Firstly, protons represent the transported substrate that collapses  $\Delta\tilde{\mu}_{H^+}$  and, secondly, protons enhance the inhibition of their own transport due to the pH dependence of PN binding. This can result in a more complex regulation in the mosaic domains: at higher  $\Delta\tilde{\mu}_{H^+}$ , the more acidic vicinity of UP potentiates the closed state and more alkaline pH resulting from decoupling lowers PN inhibition and intensifies the uncoupling state. Also, different local PN concentrations would result in different states of coupling in different domains.

A distinct modulator is  $\Delta\psi$ , which possesses a feedback character, as the final magnitude of  $\Delta\psi$  results from overall established ionic fluxes across the membrane including  $H^+$  transport through UP. We showed the nonexistence of voltage gating of the  $H^+$  channel (Fig. 5A; cf. Klingenberg and Winkler, 1985). However, a break in the  $\Delta\psi$  dependence was observed in the presence of GDP (Fig. 5A). Either GDP gating is voltage dependent (Nicholls *et al.*, 1984) or at higher  $\Delta\psi$  a leak is opened that significantly contributes to the observed  $H^+$  permeability. In the former case,  $\Delta\psi$  would be an inherent feedback modulator of PN inhibition and, in the latter case, it would



modulate coupling but not PN inhibitory ability. In this case, BAT mitochondria in the presence of GDP should exhibit a related nonohmic conductance as was found in other types of mitochondria or in vesicles from mitochondrial and other lipids (Krishnamoorthy and Hinkle, 1984; Gutknecht, 1984) as was actually observed (Nicholls, 1977; Rial *et al.*, 1983; Nicholls *et al.*, 1984). The break seen in our  $\Delta\psi$  dependence measured with GDP lies much lower than those obtained under the respiration. This could be due to an impairment of membrane  $H^+$  permeability caused by the loading procedure used. Therefore, at present, we cannot distinguish between this and the real sensitivity of PN gating to  $\Delta\psi$ . In any case, however, we can consider  $\Delta\psi$  as the feedback modulator of coupling in BAT mitochondria.

We further demonstrated a decrease in the ATP inhibitory ability at millimolar  $Mg^{2+}$  concentrations, confirming that free nucleotides rather than their  $Mg^{2+}$  complexes are required for the inhibition of UP transport (Nicholls, 1979). Therefore,  $Mg^{2+}$  was recognized as the real modulator of PN inhibition, which sets up the inhibition to the proper level.

*Possible Initiation of Thermogenesis by a Decrease in ATP Level in the Presence of Fatty Acids*

Assuming that pH in BAT cells is  $>7.1$ , we demonstrated that a decrease in ATP level in the presence of FFA is sufficient for opening the  $H^+$  channel of UP and consequently for the initiation of thermogenesis. We showed that, at ATP concentrations found *in vivo* before and after norepinephrine (La Noue *et al.*, 1986), nearly full- and about half-maximum inhibition takes place, respectively, only when  $Mg^{2+}$  is absent. With  $Mg^{2+}$ , there is no possibility of achieving full inhibition of  $H^+$  transport even at 2 mM ATP. Therefore, we must expect that *in vivo* FFA must be catabolized or that  $Mg^{2+}$  must be eliminated to attain a fully coupled state. This must also be due to the above discussed effects of  $\Delta\psi$ . In conclusion we would like to claim that both levels of regulation of  $H^+$  transport through the uncoupling protein—regulation by PN and by FFA—are equally meaningful and, under a proper setting of PN inhibitory ability by pH and  $Mg^{2+}$ , they initiate and terminate thermogenesis in BAT.

*The Uncoupling Protein as a Complex of Two Channels Regulated from a Single Purine Nucleotide Binding Site*

Our results further extended knowledge about the molecular mechanism of transport through UP. The pH optimum of  $H^+$  transport in the absence of  $Cl^-$  transport observed near pH 7 reflects identical kinetic properties of putative inner and outer  $H^+$  binding-translocating sites. At acidic pH, the dissociation of  $H^+$  from the outer site is suppressed by a high  $H^+$

concentration in the surroundings; at an alkaline outer pH, there is an equilibration of pH gradient before valinomycin addition in our experimental setup. It proceeds as slow  $H^+$  extrusion and, consequently, the protonated inner  $H^+$  binding site cannot rapidly accept  $H^+$  driven by  $K^+$  diffusion potential. Therefore, it results in a decrease in the transport rate.

Such a pH optimum is not observed and  $H^+$  transport is even accelerated (except at neutral pH) when simultaneous  $Cl^-$  uptake proceeds (Fig. 9). This can be explained on the basis of a faster utilization of the common driving force when ions of opposite sign move across the membrane in opposite directions. This explanation explicitly assumes the independence of such ion transport pathways, and this finding provides the evidence for the different structural natures of  $H^+$  and  $Cl^-$  channels within the UP dimeric unit, which are also supported by the following findings:  $H^+$  extrusion proceeds asynchronously with  $Cl^-$  uptake (Fig. 1).  $H^+$  extrusion is less sensitive to PN inhibition than is  $Cl^-$  uptake due to the existence of the latent concentration range, whereas the binding site exhibits a single dissociation constant (Figs. 1, 3B, and 4, and Tables I and II).  $H^+$  extrusion shows a pH optimum while  $Cl^-$  transport does not. Only  $H^+$  transport is inhibited by the removal of endogenous FFA (Fig. 7). In addition to data presented here, definitive support derives from the finding of SH groups essential exclusively for  $H^+$  translocation, but not for  $Cl^-$  translocation, via UP (Ježek, 1987).

A correlation between GDP inhibition and a simple model extended only by a consideration that the interaction starts above a threshold concentration (Table II) supports the existence of a single regulatory PN binding site within the complex of two channels.

All of our considerations can be summarized in a model of structural domains of UP (Fig. 10) exhibiting the following features:

1. UP forms two structurally different pathways for  $H^+$  and  $Cl^-$  translocation: an  $H^+$  channel and a  $Cl^-$  channel.<sup>5</sup>
2. Both pathways are differentially controlled via the common PN binding site— $H^+$  transport is less sensitive.
3. Only the  $H^+$  channel possesses a separate gate<sup>6</sup> controlled by FFA, which opens when FFA are bound to a putative FFA-binding site of UP. This gate is probably placed in series with the PN-controlled gate in the  $H^+$  channel.

<sup>5</sup>The term *channel* could define a transport pathway in which amino acid residues ensuring the specificity are accessible from both sides of the membrane. The *carrier* should describe a transport pathway with at least two different specific binding sites localized at the opposite sides or one reorientating site for translocated substrate. From this point, the UP should be characterized as a carrier. To save text space, however, we used the term channel in the broad sense of the word as a transport pathway.

<sup>6</sup>The term *gate* designates protein residues directly involved in inhibition of transport.

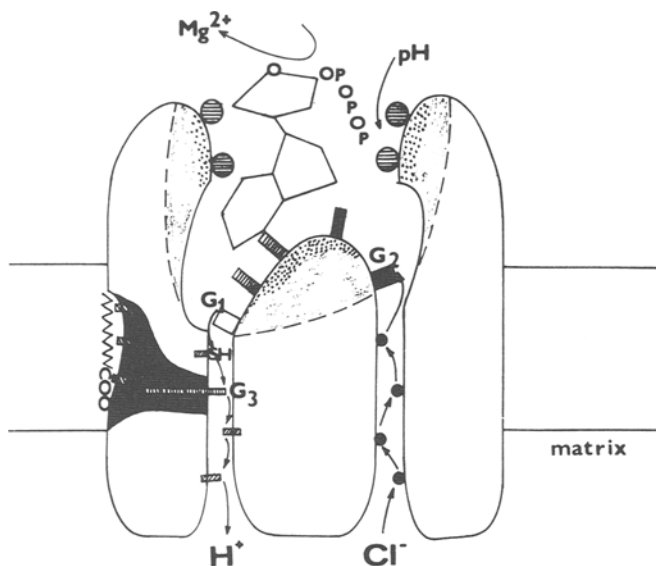


**Fig. 10.** Putative view of the uncoupling protein and location of sites of regulatory ligand binding and interaction of modulators. Our model of UP domains considers two distinct transport pathways for translocation of  $H^+$  and  $Cl^-$ , respectively: a purine nucleotide-controlled gate (enlarged) containing single gates closing the channels ( $G_1$ ,  $G_2$ ), and a purine nucleotide-binding site (dotted areas) containing various amino acid residues (the rectangles and squares) interacting with nucleotide molecule. A separate gate ( $G_3$ ) mediates the activating effect of free fatty acids (it allows  $H^+$  translocation only when FFA is bound to FFA-binding site). This gate and the FFA-binding site are drawn as the black area.

4. The PN-binding site is a complicated structure (cf. Ježek *et al.*, 1988) allowing the binding of uncomplexed nucleotides and the differential gating of  $H^+$  and  $Cl^-$  channels—ensuring gating of the  $H^+$  channel only above some threshold concentration (conformational changes of the PN-binding site could be responsible for it) and decreasing the binding and, consequently, the gating at alkaline pH and probably also at higher  $\Delta\psi$ . The pH effect can result from pH-dependent interaction of some atoms in the nucleoside with an amino acid residue of the PN binding site when either some functional groups of the nucleotide or of the protein are protonated.

### Acknowledgments

The authors thank Dr. Arnošt Kotyk for critical reading of the manuscript of the article. The expert technical assistance of Ms Natálie Hánová and Ms Věra Fialová is gratefully acknowledged.

## References

- Cannon, B., and Nedergaard, J. (1985a). *Essays Biochem.* **20**, 110–164.
- Cannon, B., and Nedergaard, J. (1985b). In *New Perspectives in Adipose Tissue: Structure, Function and Development* (Cryer, A., and Van, R. L. R., eds.), Butterworths, London, pp. 223–270.
- Cannon, B., Sundin, U., and Romert, L. (1977). *FEBS Lett.* **74**, 43–46.
- Chinet, A., Friedli, C., Seydoux, J., and Girardier, L. (1978). *Experientia*, **32**, Suppl. 25–32.
- Drahota, Z., Houštěk, J., Ježek, P., Kopecký, J., Rauchová, H., and Rychter, Z. (1985). In *Proceedings of the 16th FEBS Congress Part A* (Ovchinnikov, Yu., ed.), VNU Science Press, The Netherlands, pp. 511–518.
- Fergussion, S. J. (1985). *Biochim. Biophys. Acta* **811**, 47–95.
- Gutknecht, J. (1984). *J. Membr. Biol.* **82**, 105–112.
- Heaton, G. M., Wagenvoort, R. J., Kemp, A., Jr., and Nicholls, D. G. (1978). *Annu. Rev. Nutr.* **5**, 69–94.
- Hittelman, K. J., Lindberg, O., and Cannon, B. (1969). *Eur. J. Biochem.* **11**, 183–192.
- Houštěk, J., Ježek, P., and Kopecký, J. (1987). In *Membranes and Receptor Mechanism* (Bertoli, E., Cambria, A., Scampagnini, V., and Chapman, D., eds.), Fidia Research Series, Vol. 7, Liviana Press, Padova, pp. 177–191.
- Ježek, P. (1987). *FEBS Lett.*, **211**, 89–93.
- Ježek, P., Houštěk, J., Kotyk, A., and Drahota, Z. (1988). *Eur. Biophys. J.* (in press).
- Klingenberg, M. (1984). *Biochem. Soc. Trans.* **12**, 390–393.
- Klingenberg, M., and Winkler, E. (1985). *EMBO J.* **4**, 3087–3092.
- Kopecký, J., Guerrieri, F., Ježek, P., Drahota, Z., and Houštěk, J. (1984). *FEBS Lett.* **170**, 186–190.
- Kopecký, J., Ježek, P., Drahota, Z., and Houštěk, J. (1987). *Eur. J. Biochem.* **164**, 687–694.
- Krishnamoorthy, G., and Hinkle, P. C. (1984). *Biochemistry* **23**, 1640–1645.
- La Noue, K. F., Strzelecki, I., Strzelecka, D., and Koch, C. (1986). *J. Biol. Chem.* **261**, 298–305.
- Lin, C. S., and Klingenberg, M. (1982). *Biochemistry* **21**, 1082–1089.
- Locke, R. M., Rial, E., Scott, I. D., and Nicholls, D. G. (1982). *Eur. J. Biochem.* **129**, 373–380.
- Mewes, H. W., Rafael, J. (1981). *FEBS Lett.* **131**, 7–10.
- Nicholls, D. G. (1974). *Eur. J. Biochem.* **49**, 573–583.
- Nicholls, D. G. (1977). *Eur. J. Biochem.* **77**, 349–356.
- Nicholls, D. G. (1979). *Biochim. Biophys. Acta* **549**, 1–29.
- Nicholls, D. G., and Lindberg, O. (1973). *Eur. J. Biochem.* **37**, 523–530.
- Nicholls, D. G., and Locke, R. M. (1984). *Physiol. Rev.* **64**, 1–64.
- Nicholls, D. G., Cannon, B., Grav, H. J., and Lindberg, O. (1974). In *Dynamics of Energy Transducing Membranes* (Ernster, L., Estabrook, R., and Slater, E. C., eds.), Vol. 13, Elsevier, Amsterdam, pp. 529–537.
- Nicholls, D. G., Snelling, R., and Rial, E. (1984). *Biochem. Soc. Trans.* **12**, 388–390.
- Norman, P. T., and Flatmark, I. (1984). *Biochim. Biophys. Acta* **794**, 225–233.
- Rial, E., Poustie, A., and Nicholls, D. G. (1983). *Eur. J. Biochem.* **137**, 197–203.
- Slavík, J., and Kotyk, A. (1984). *Biochim. Biophys. Acta* **766**, 679–684.
- Strieleman, P. J., and Shrago, E. (1985). *Am. J. Physiol.* **248**, E699–E705.
- Strieleman, P. J., Schalinske, K. L., and Shrago, E. (1985a). *Biochem. Biophys. Res. Commun.* **127**, 509–516.
- Strieleman, P. J., Schalinske, K. L., and Shrago, E. (1985b). *J. Biol. Chem.* **260**, 13,402–13,405.
- Warhurst, I. W., Dawson, A. P., and Selwyn, M. J. (1982). *FEBS Lett.* **149**, 249–252.
- Westerhoff, H. V., Melandri, B. A., Venturoli, G., Azzone, G. F., and Kell, D. B. (1984). *Biochim. Biophys. Acta* **768**, 257–292.